Available online at www.sciencedirect.com
SCIENCE DIRECT
Engineering Structures 28 (2006) 783–792
ENGINEERING STRUCTURES
www.elsevier.com/locate/engstruct

Validated analysis and strengthening of a 19th century railway bridge

John Ermopoulos[a], Constantine C. Spyrakos[b,*]

[a] *Department of Civil Engineering, Laboratory of Metal Structures, National Technical University of Athens (N.T.U.A.), 42 Patission Street, 10682, Athens, Greece*
[b] *Department of Civil Engineering, Earthquake Engineering Laboratory, National Technical University of Athens (N.T.U.A.), Zografos 15700, Athens, Greece*

Received 3 November 2003; received in revised form 17 May 2005; accepted 12 October 2005
Available online 5 December 2005

Abstract

A systematic study of a historic railway steel truss bridge, still in use, is presented. The study includes static and dynamic field measurements as well as laboratory tests. The tests have been conducted to develop a validated analytical model, which in turn is employed to assess the capacity of the bridge to carry heavier train loads as well as seismic and wind loads, as specified by current codes. Members that require strengthening or replacement are identified, strengthening schemes are proposed and the remaining fatigue life of the bridge in its present condition and after the suggested strengthening is predicted.

Keywords: Railway steel bridge; Field measurements; Bridge strengthening

1. Introduction and historic background

Assessment of the current condition of steel railway bridges is of increasing interest both in the US and Europe [1–4]. Many of these studies combine analysis with experiments in order to evaluate the behavior of the bridges and arrive at design recommendations and retrofit schemes [5–8]. One of the main reasons for the increased interest and frequency in published work is lack of funding to replace aging steel bridges in conjunction with increasing demand on railway traffic, facts that spurred the present investigation.

At the end of the 19th century the Greek government developed a railway network in the southern part of Greece. Since this area is mostly mountainous, a large number of steel railway bridges with 10 to 60 m spans were constructed along this network. Their design and construction started in 1890 according to French codes and with the co-operation of a French company. Selective strengthening and replacement of members, such as secondary beams, parts of the main beams and bracings, was performed in 1944 and mostly in 1963 in order to meet increased traffic loads.

Record files and practices of the Greek Railway Organization (GRO) indicate meticulous and consistent periodic inspection and maintenance of the bridges. Since the majority of these bridges are in use today, in 2002 the owner of the whole railway network (i.e., the GRO) decided to evaluate their condition and identify necessary strengthening to bring them up to modern standards, while respecting the historic fabric of the bridges. The project also included strengthening schemes and bridge member replacement based on the extent and cost of the required upgrade. The present work presents salient features of the procedure as well as the results of an extensive study on a particular and characteristic deck-truss bridge of this railway network (Fig. 1). The bridge was designed and built by the French company "Societé Anonyme Internationale de Construction et d' Entreprice de Traveaux Publics". Construction started in 1889 and was completed in

Fig. 1. General view of the steel bridge.

* Corresponding author. Tel.: +30 210 7721187; fax: +30 210 6990044.
E-mail address: spyrakos@hol.gr (C.C. Spyrakos).

0141-0296/$ - see front matter © 2005 Elsevier Ltd. All rights reserved.
doi:10.1016/j.engstruct.2005.10.006

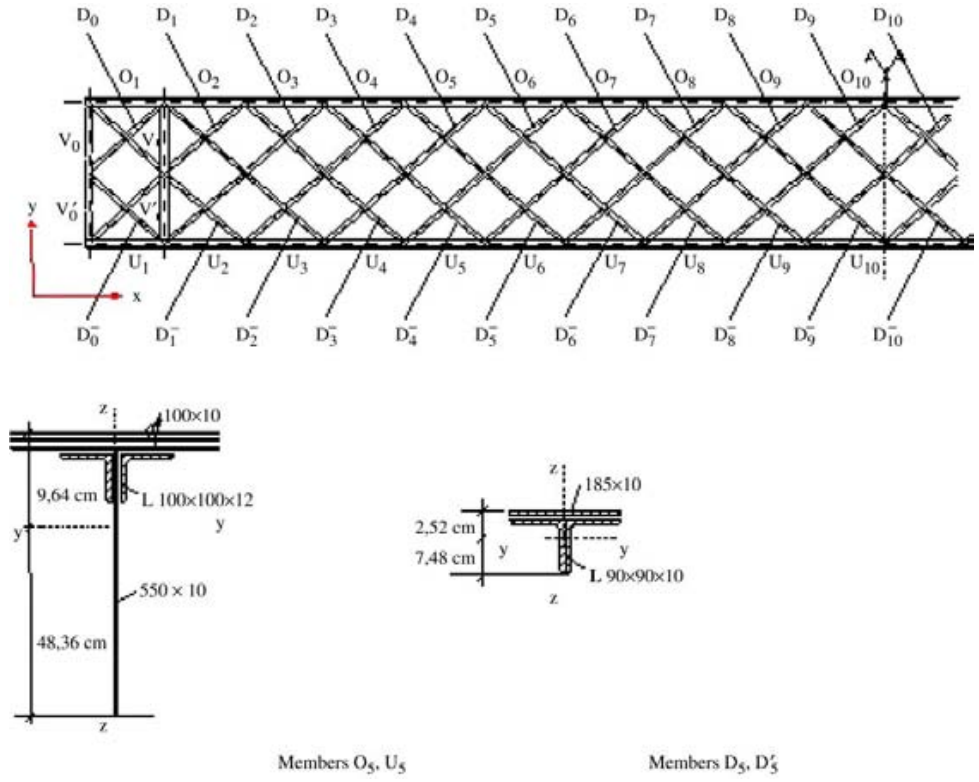

Fig. 2. Main truss girder and representative cross-sections.

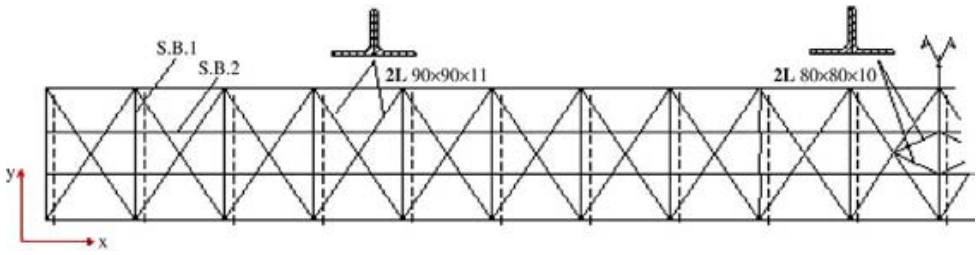

Fig. 3. Horizontal bracing system in the upper chord and secondary beams.

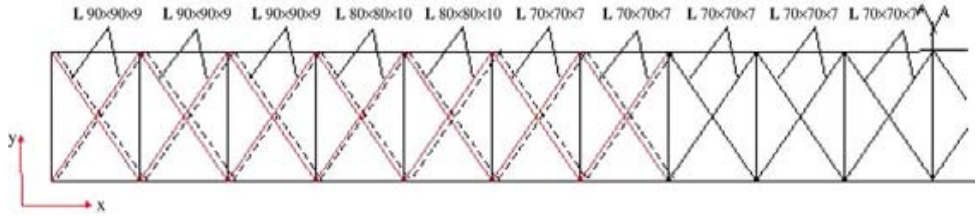

Fig. 4. Horizontal bracing system in the lower chord.

1896. The project is an achievement even with 20th century constructional technology.

2. Bridge description

As shown in Fig. 1, the seven span bridge is symmetric with the six spans made of masonry, while the central span is a 51.60 m long steel superstructure. The main girders are two riveted parallel trusses 5.20 m high and 3.40 m apart; see Fig. 2. As shown in Fig. 2, the main truss girder consists of combined plates and L sections. At the upper chord, the main trusses are connected with the horizontal bracing system and the longitudinal secondary beams shown in Fig. 3. Also, at the center of the upper chord, the bridge is further stiffened with the braking–acceleration bracing system shown in Fig. 3. At the lower chord the bracing system and members are depicted in Figs. 4 and 5. The vertical transverse bracing is strengthened at the two ends as shown in Fig. 6. In Figs. 3, 4 and 6, dash lines have been used to indicate the members that,

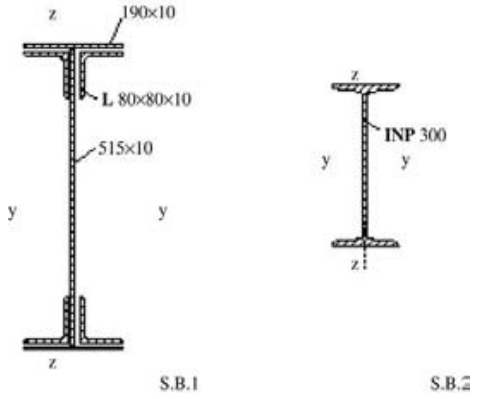

Fig. 5. Cross sections of secondary beams (S.B. 1 and S.B. 2).

according to the analysis elaborated in the following sections, need to be strengthened. A representative connection of the bracing system at the lower chord is shown in Fig. 7. The 20-panel bridge superstructure is simply supported through two restraining and two roller bearings on massive unreinforced masonry piers.

3. Field and laboratory testing

As a part of this research, extensive field-testing, laboratory testing and analytical work were performed to assess the condition of the superstructure, and propose a strengthening scheme, a procedure successfully used by the authors to assess the condition of several bridge structures, e.g. Spyrakos, Kemp and Venkatareddy [9,10].

The in situ measurements of member sizes, connections and support bearings verified the fact that the existing drawings were applied and only a few insignificant variations were observed.

Table 1
Vertical deflections in cm at midspan

Position of engine truck [Φ_i]	Measured	Analytical
Φ_1	0.400	0.443
Φ_2	0.800	0.646
Φ_3	1.100	1.246
Φ_4	1.100	1.410
Φ_5	1.200	1.589
Φ_6	1.500	1.677
Φ_7	1.500	1.666
Φ_8	1.500	1.673

In situ measurements were performed using an 800 kN engine track [11]. The in situ measurements were carried out by a team headed by Professor P. Karydis (Director of the Laboratory for Earthquake Engineering at N.T.U.A.). Specifically, the bridge was instrumented with strain gages placed at selected locations to measure normal stresses, as shown in Figs. 8 and 9. In Fig. 8 Φ_i ($i = 1$ to 8) indicates the position of the first axle of the six-axle engine truck. The distances between the axles are also shown in Fig. 8. During field-testing, the horizontal along the longitudinal and transverse axes as well as the vertical vibrations were recorded with accelerometers having a sensitivity of 10 V/g placed near the midspan of the bridge (Fig. 10). In order to measure the free-vibration, accelerations were recorded after the 800 kN engine had crossed the bridge. Strains were also recorded for trains that crossed the bridge in order to assess the behavior of the superstructure for currently used trains. These measurements were performed twice: once for each direction of the traveling train. The speed of the 800 kN engine track as well as the regular trains were measured with geophones having a sensitivity of 28.8 V/m/s, (Fig. 11).

Moreover, the vertical deflections near the midspan were mechanically measured by appropriate device. Tables 1 and 2

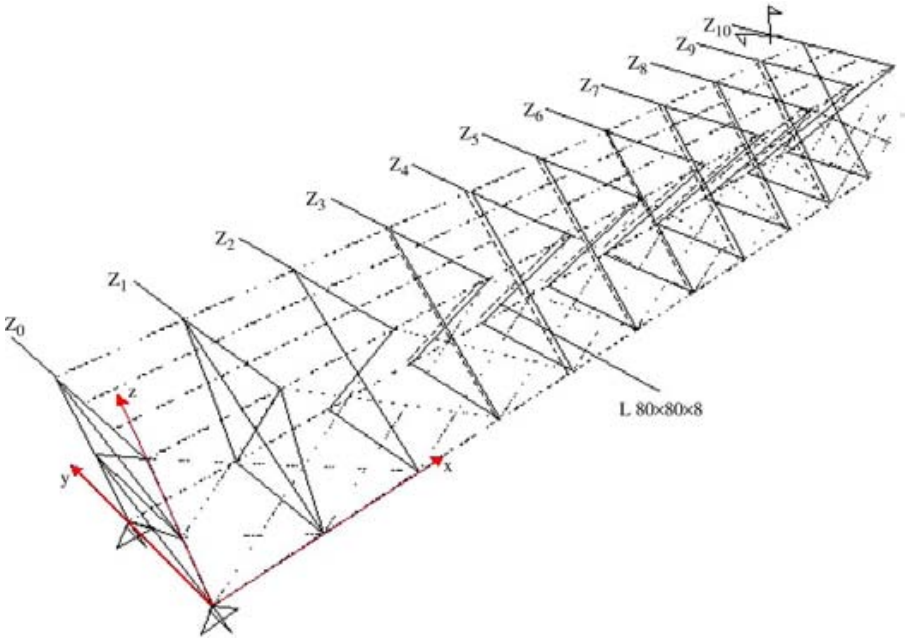

Fig. 6. Vertical transverse bracings.

Table 2
Eigenperiods in s of steel superstructure

Normal modes	Recorded	Analytical
1	0.227	0.202
2	0.078	0.081
3	0.067	0.059

Fig. 7. Connection of the bracing system at the lower chord.

list the vertical deflections caused by the 800 kN engine at the midspan of the bridge and the lowest three eigenperiods extracted from the records during free vibration in the vertical direction, respectively.

Laboratory tests, such as tension tests, chemical analysis and fatigue tests, were also carried out on specimens extracted from representative members that are prone to fatigue [12]. Specifically, specimens were extracted from the webs of the upper and lower chord of the main girder and from the web of the transverse beams, and the members were fully restored with riveted plates as shown in Fig. 12.

Table 3
Results in % of volume from chemical analysis

Specimens	C	Si	Mn	P	S
No. 1	0.084	>6.36	0.034	>0.160	>0.110
No. 2	0.061	5.18	0.062	>0.160	>0.110
No. 3	0.042	<0.01	0.390	0.022	0.015
No. 4	0.038	<0.01	0.390	0.023	0.015

Tension tests indicated that member material partially complied with the St37-2 requirements [13]. Inadequacies were observed regarding the ultimate tensile strength and corresponding elongation. Chemical analysis indicated the use of different steel grades for the main girder trusses and the secondary beams, the former being of superior quality than the latter. The results from the chemical analysis are presented in Table 3.

From Table 3 it is obvious that the specimens No. 1 and No. 2, which are extracted from the truss girder, correspond to an old material, while the specimens No. 3 and No. 4, which are extracted from the transverse beams, correspond to a new material that replaced the old one 30 to 40 years ago. Metallographic tests showed that member material is perlite–ferritic steel with several oxides and sulfides [12].

In order to estimate the dynamic allowance factor, the same engine was passed over the bridge with three different speeds, i.e., 10 km/h, 30 km/h and 50 km/h. The records for regular trains were collected for a 10 km/h speed, restrained by the speed limit set for the field measurements [11].

Specimens were also used to perform fatigue tests. The results of the tests are shown in Figs. 13 and 14. In these figures the curve corresponding to detail category 112 of Eurocode 3 was introduced [14]. In both figures the fatigue strength of

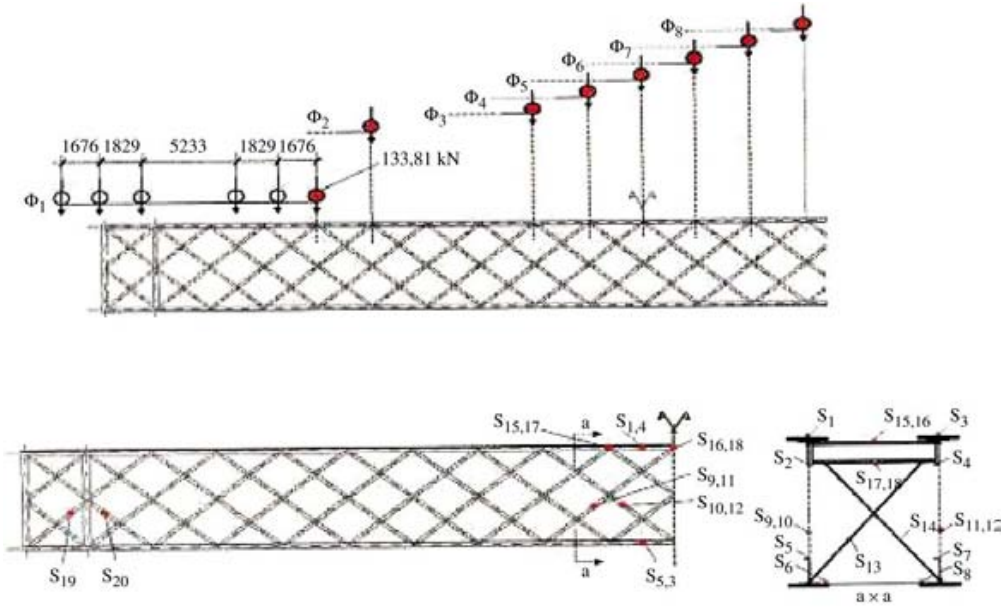

Fig. 8. Positions of the engine truck [Φ_i] and positions of strain gages [S_i].

Fig. 9. Strain gage placed at location S_{18}.

Fig. 10. Horizontal and vertical accelerometers.

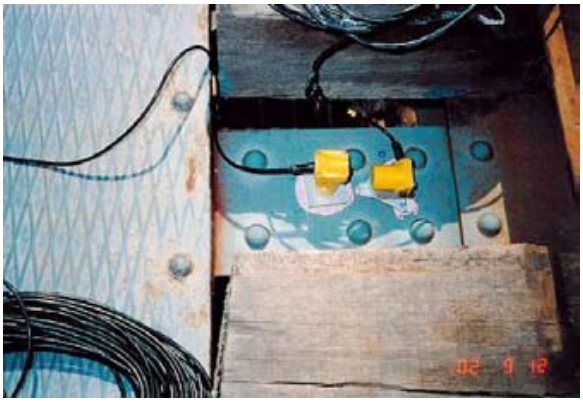

Fig. 11. Horizontal and vertical geophones.

Fig. 12. Details from the locations of the extracted pieces.

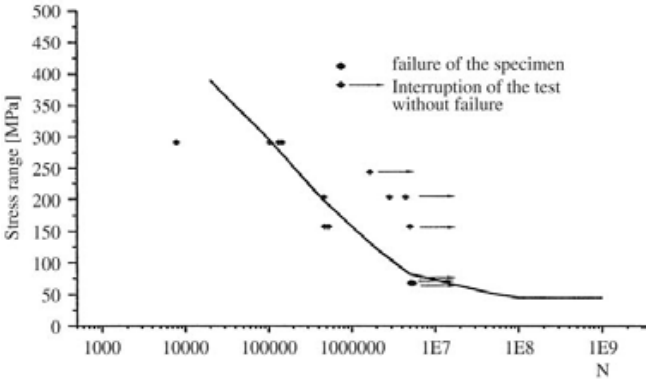

Fig. 13. Results from fatigue tests for the main girder.

the tested material could be classified at least at this detail category.

4. Validation of analytical model

Because of the high degree of indeterminacy of the truss-system, a finite element analysis was employed to study the response of the structure. The bridge is modeled with three-dimensional (3-D) beam elements conforming to the guidelines given in [15]. Although the structural system is a truss system, all joints of the model are modeled as rigid connections according to the design specifications in [8]. A typical connection of vertical studs, diagonal ties and top beam of the truss system that justifies the rigid joint modeling is shown in Fig. 7. As a consequence, moments are transferred through joints and are proven to be of interest only for the top and bottom beams of the trusses as well as for the floor and deck beams. In the main girders, the moments that develop in the vertical posts and the diagonals are negligible.

The dynamic analysis of the system was based on a lumped mass formulation [15]. The following assumptions were made: (i) the loads and reactions are applied only at joints, and, (ii) besides the lumped masses generated at the nodes to simulate

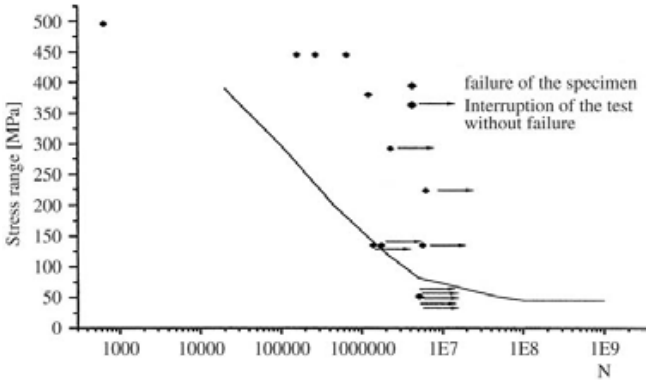

Fig. 14. Results from fatigue tests for the transverse girder.

the inertia of the members, additional masses are introduced at the deck beams to account for the deck loads.

The material properties of the structural steel used for the members were obtained by in situ and laboratory measurements [12]. The measured modulus of elasticity is $E = 2.1 \times 10^8$ kN/m^2, the yield stress is $f_y = 28.50$ kN/cm^2, and the ultimate stress is $f_u = 30.80$ kN/cm^2. Based on the test results, the allowable stress for tension, compression and bending is taken as $\sigma_a = 15.67$ kN/cm^2, whereas the allowable shear stress is taken as $\tau_a = 9.04$ kN/cm^2.

In order to assess the accuracy of the 3-D finite element model used in the analysis, the results from the analytical calculations were compared with those obtained from the field measurements. In the analytical procedure the normal stresses were calculated at the same locations where the strain gages were placed (Fig. 8, locations S_i). For each position of the engine truck [Φ_i] ($i = 1$ to 8) the corresponding stresses and the vertical deflections at midspan were calculated analytically. Table 1 lists the deflections at midspan computed with the FE model and the in situ measured values for the test engine truck. As indicated in Table 1 the measured and the computed deflections are practically identical.

The first three eigenperiods of the 3-D finite element model of the system are listed in Table 2, while the corresponding mode shapes are drawn in Fig. 15. The measured and the calculated eigenperiods are practically identical. Such correlation clearly indicates the validity of the FE model.

In Figs. 16 and 17 the stresses calculated from the analysis and those obtained through strain gages at indicative locations are shown. The differences are not significant. However, conservatism in the calculations with the finite element model is preserved, since in most cases the analytical results are greater than the corresponding measured values.

5. Analysis and strengthening of members

Design calculations with the aid of the validated 3-D model of the bridge were performed for the loading combinations in order to assess the strength, stability and functionality of the bridge for the train types specified by the owner. The loads for the analysis, such as wind loads, traction and braking forces, nosing force and eccentricity of vertical loads, were applied according to the German Codes DS804 [16].

The earthquake load was applied according to the Greek Aseismic Code [17]. The design acceleration spectrum, $\Phi_d(T)$,

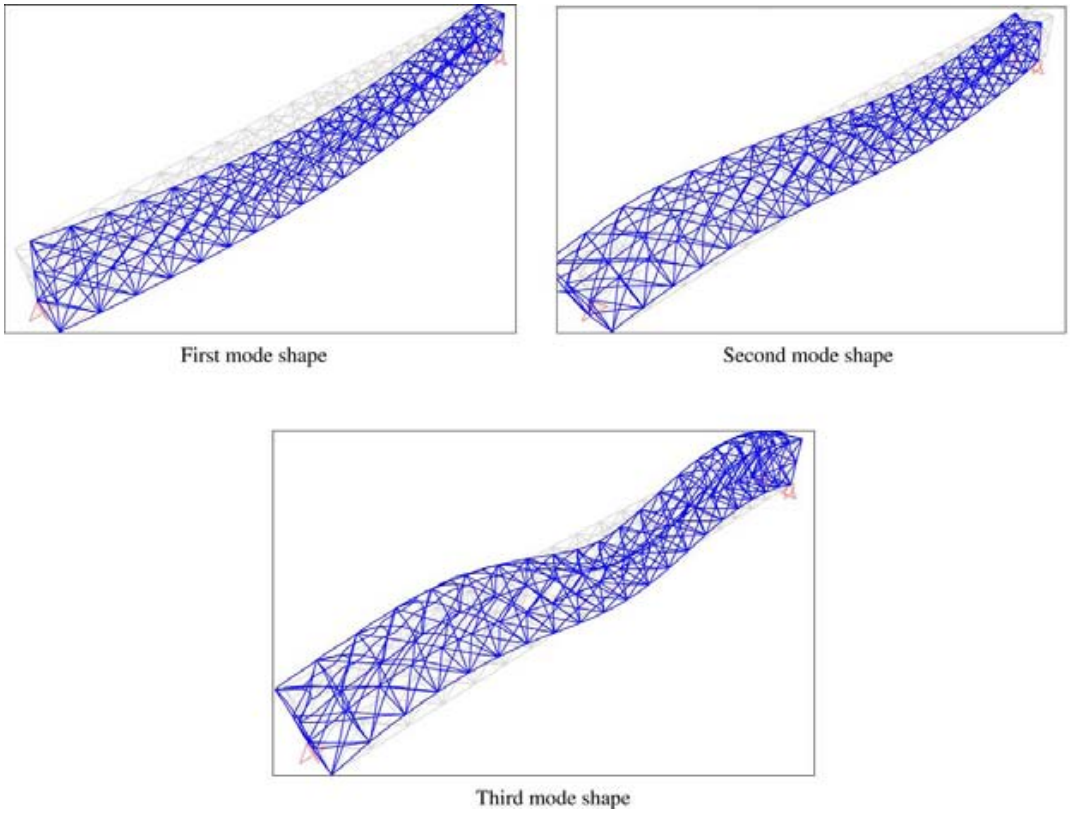

Fig. 15. First, second, and third vertical mode shapes.

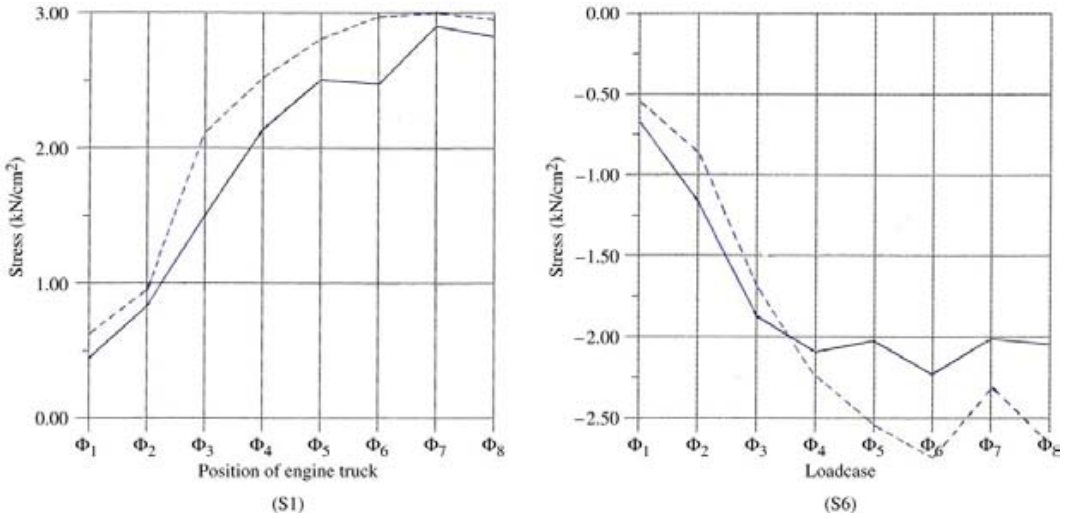

Fig. 16. Locations S1 and S6: Stress versus loading [Φi] (continuous line: tests; dashed line: analytical).

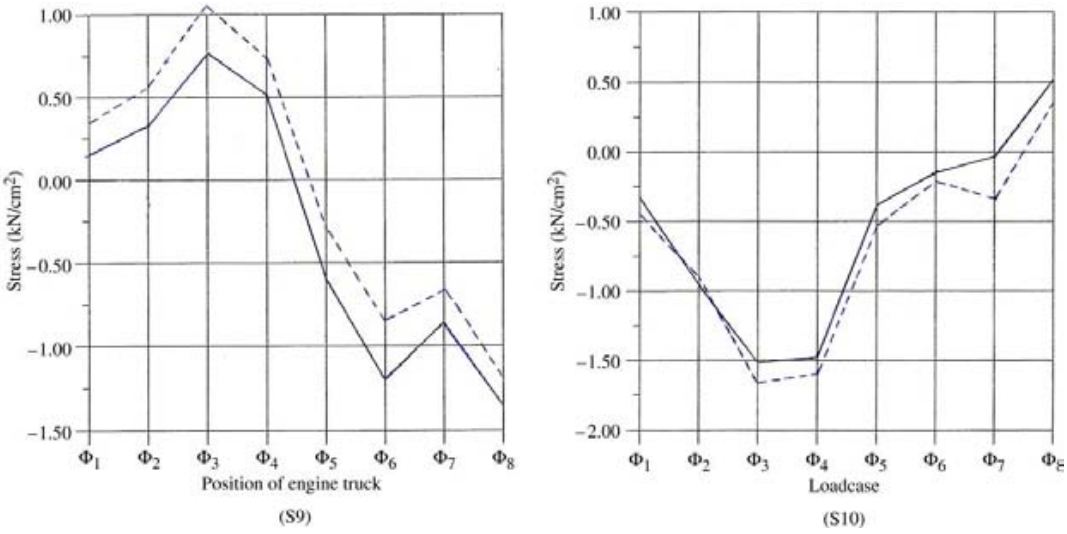

Fig. 17. Locations S9 and S10: Stress versus loading [Φi] (continuous line: tests; dashed line: analytical).

for the bridge site is shown in Fig. 18. The spectra correspond to a soil class that characterizes weathered rocks and to a seismic behavior factor, $q = 1$, which corresponds to elastic behavior. The ordinates for the design acceleration spectra are computed for each period from the following formulae for a soil class B, i.e., strongly weathered rock, with characteristic periods $T_1 = 0.15$ s and $T_2 = 0.60$ s [17].

$$0 \le T < T_1 \qquad \Phi_d(T) = 0.16g\left(1 + 1.5\frac{T}{T_1}\right)$$

$$T_1 < T < T_2 \qquad \Phi_d(T) = 0.4g$$

$$T_2 < T \qquad \Phi_d(T) = 0.4g\left(\frac{T_2}{T}\right)^{2/3}$$

The railway loads, specified by the owner, are shown in Fig. 19. Specifically, the first load model (TRAIN 1961) consists of either one or two engines (a) followed by a series of railroad cars (b), while the second (RAILBUS) consists of a minimum of one to a maximum of three railroad cars (c) CEN [18].

The design calculations for the members and the corresponding cross-sections were performed according to [13]. The connections between the members were assumed to be rigid, an assumption that was validated by the static and dynamic tests, as shown in Tables 1 and 2. The analysis of the girders and the floorbeams was performed accounting an accidental eccentricity $s = \pm 10$ cm as specified by DS804 [16]. The loads applied on each axle are shown in Fig. 20(a). The floorbeams have been analyzed for the three moving loads shown in Fig. 20(b), which are equivalent to the axle load specified by DS804 [16]. The wind load is taken as 2.50 kN/m^2 and 1.25 kN/m^2 for the unloaded and the loaded bridge, respectively, [8]. The impact load is simulated with the concentrated lateral load applied at the upper part of the rail, as shown in Fig. 20(c). In order to calculate the stresses that correspond to the lateral load, the part of

Table 4
Remaining fatigue life

Scenarios of future traffic	Secondary beams (BS2)	Secondary transversal beams (BS1)	Main girders
TRAIN 1961: Ten passages per day [2D + 5F]	40 years	20 years	40 years
RAILBUS (three railroad cars on line): Ten passages per day	40 years	20 years	40 years

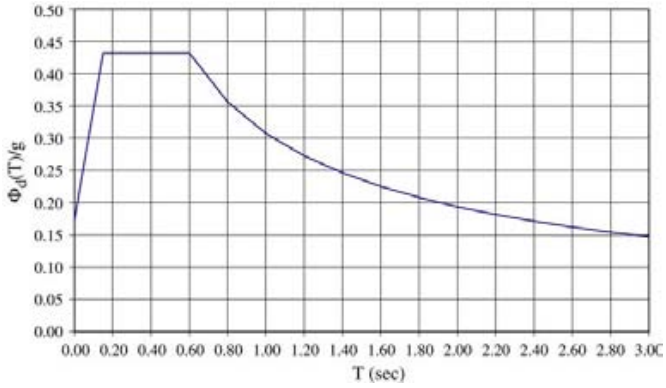

Fig. 18. Design spectrum.

the rail that lies between three successive beams of the bridge is considered. The support of the secondary beams on the floor beams is simulated with linear springs with a stiffness that has been evaluated as the inverse of the vertical deflection δ for a unit load as shown in Fig. 20(d).

Braking, acceleration and lateral loads due to impact are also calculated according to DS804. Specifically, the acceleration load $F_{x,\mathrm{An}}$ and the breaking load $F_{x,\mathrm{Br}}$ can be calculated from [16]:

$$F_{x,\mathrm{An}} = 33.3 \times L \times \xi$$
$$F_{x,\mathrm{Br}} = f_{x,\mathrm{Br}} \times L \times \xi$$

where L is the basic length of loading, which for the specific application has been taken as 51.6 m, and ξ is a reduction factor that accounts for the interaction between the axle and the rail as well as the flexibility of the supporting members in undertaking the horizontal forces $F_{x,\mathrm{An}}$ and $F_{x,\mathrm{Br}}$. In our case ξ is taken as equal to 1 and $f_{x,\mathrm{Br}} = 20$ kN/m according to [16].

The load combinations include the [H], the [HZ] and the [HZE]. For the combination [H] the dead load is added to the moving loads increased by the impact load factor φ, given the values 1.87 for the girders and the floorbeams and 1.03 or 1.17 for the other bridge members. The [HZ] combination includes the load cases: (i) the dead load (G), the moving loads (Q) increased by φ and the acceleration-braking loads, (ii) the dead load and the wind load for the unloaded bridge, (iii) the dead load, the moving loads increased by φ and the wind load for the loaded bridge and (iv) the dead load, the moving loads increased by φ, the wind load for the loaded bridge and the acceleration–braking loads. The [HZE] combination includes the dead load, 30% of the moving loads increased by φ and the seismic loads (E). Specifically, the [HZE] consists of the following spatial superposition combinations [17]:

$$G + \psi_2 \varphi Q \pm E_x \pm \lambda E_y \pm \mu E_z$$
$$G + \psi_2 \varphi Q \pm \lambda E_x \pm E_y \pm \mu E_z$$
$$G + \psi_2 \varphi Q \pm \lambda E_x \pm \mu E_y \pm E_z$$

where the load combination factor $\psi_2 = 0.3$ and $\lambda = \mu = 0.3$

In addition fatigue calculations were performed using a load history and future loads given by the GRO [8,19]. The calculations were based on real material properties obtained from the tests. The great variety of axle loads was tackled by categorizing them into three groups, that is 7.5 t, 10 t and 14 t axle loads, respectively. The loading cycles n for the 110 year service life of the bridge, the stress range $\Delta\sigma$ for each group of axle loads and the corresponding number of cycles N from the diagrams given in EC3 [14] and EBETAM [12] were calculated. It has to be noted that data for the load history of the bridge were not available before the Second World War, and as a result mean values were used for this period.

The analysis and the design calculations showed that for the new train types, i.e., TRAIN 1961 and RAILBUS, strengthening in various members was necessary. Such members are located in the upper and lower chord as well

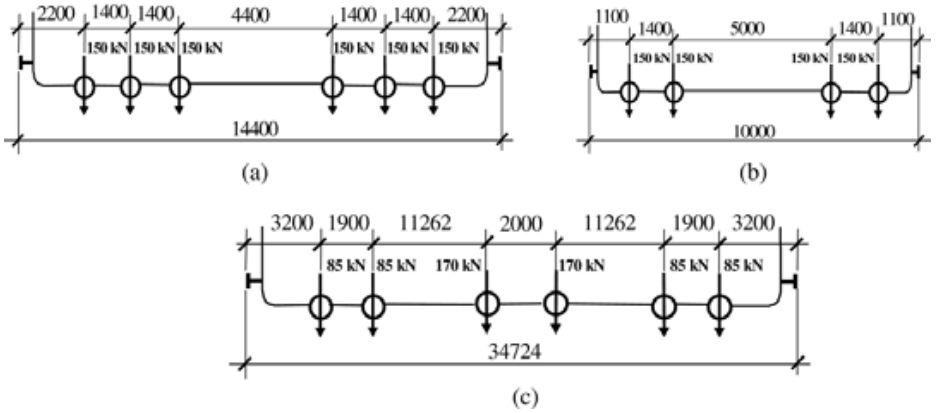

Fig. 19. TRAIN 1961 (a) engine and (b) railroad car; (c) RAILBUS.

as on the vertical transverse bracing shown with dashed lines in Figs. 3, 4 and 6, respectively. Fig. 20 demonstrates strengthening of a representative transverse beam through riveting of steel plates to the upper and lower flanges of the bridge member. The type of strengthening is also indicated in Figs. 21 and 22 that is the reciprocal of Fig. 4. Strengthening can be obtained through additional steel plates riveted to the flanges. Riveting is suggested for aesthetics.

Regarding the remaining fatigue life of the various parts of the bridge after the suggested strengthening of the members the Miner–Palgrem criterion ($\sum \frac{n}{N} \leq 1$) was applied [19]. The results for various scenarios are presented in Table 4.

6. Final results and conclusions

On the basis of the experimental and analytical procedure, the final results and conclusions for the bridge under consideration are the following.

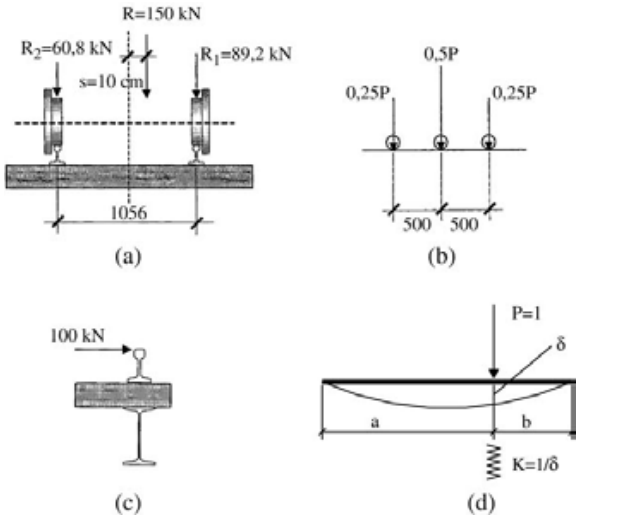

Fig. 20. (a) Loads from accidental eccentricity. (b) Loading on floorbeams. (c) Impact loads. (d) Analytical model.

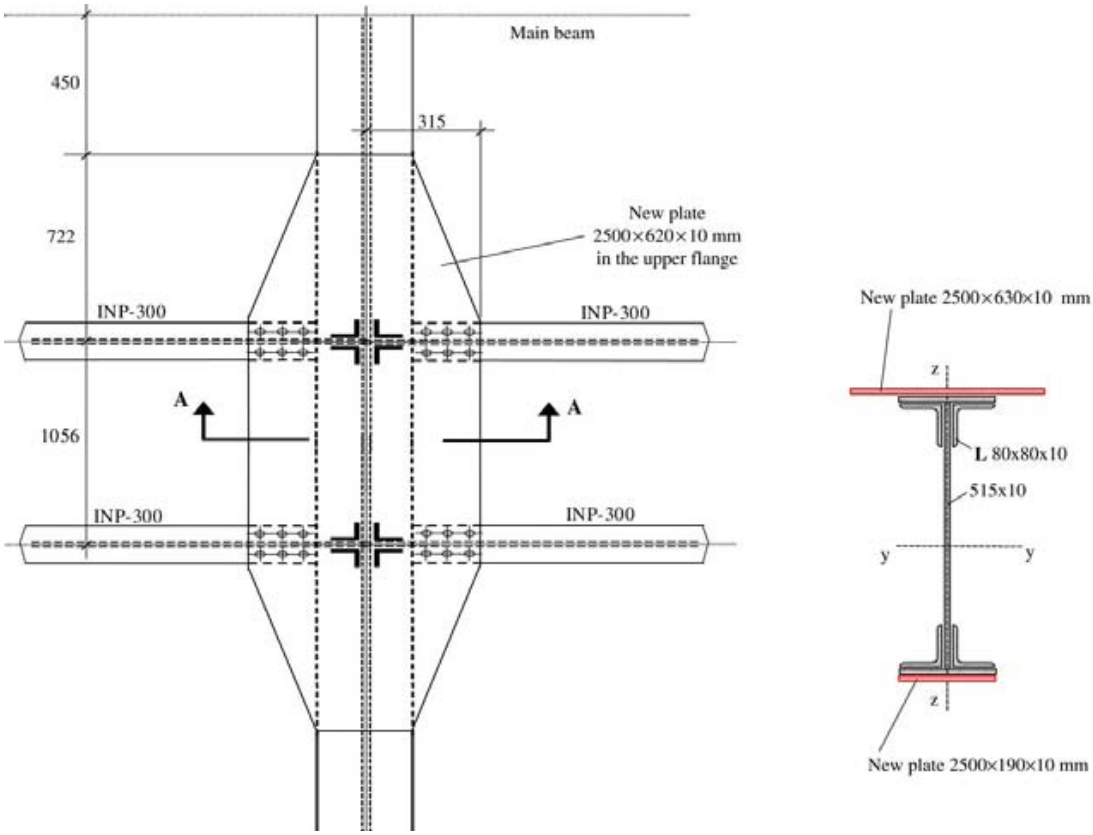

Fig. 21. Strengthening of the transverse secondary beams.

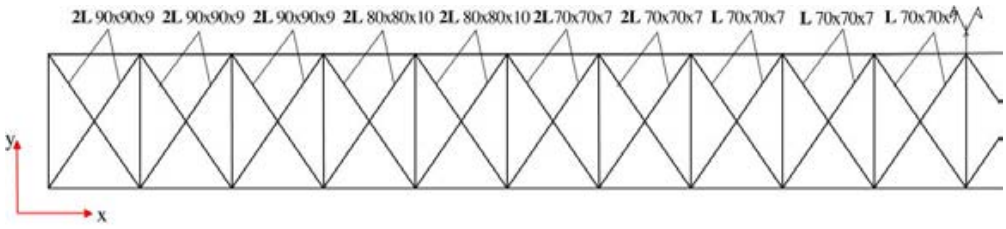

Fig. 22. Horizontal bracing system in the lower chord (strengthened).

- The existing geometry and dimensions of the bridge are in almost full agreement with those included in the original drawings. However, a few minor differences that were identified were also considered in the analysis.
- The analysis and design for the new train types indicated that strengthening is required in various elements of the bridge, primarily in the lower chords and in the transverse bracing system.
- Interruption of traffic during strengthening works on the bridge is not considered as a hindrance because the members that need strengthening are not directly connected to the rail tracks, excluding the transverse beams, for which a procedure could be devised to minimize traffic interruption.
- The relatively good condition of the bridge is primarily attributed to the systematic and periodic inspection and maintenance. In conclusion, the bridge can continue to be in service and with the suggested strengthening it can safely fulfill the design requirements and future needs of the GRO.

Acknowledgement

The authors wish to express their sincere appreciation to the Greek Railway Organization for the financial support of this pilot project.

Appendix

The following symbols are used in this paper:

E = Young's modulus;
f_y = yield stress;
f_u = ultimate stress;
σ_a = allowable stress for tension, compression and bending;
τ_a = allowable shear stress;
$\Phi_d(T)$ = design acceleration spectrum;
q = seismic behavior factor;
C = carbon;
Si = silicon;
Mn = manganese;
P = phosphorus;
S = sulfur.

References

[1] Tobias DH, Foutch DA, Choros J. Loading spectra for railway bridges under current operating conditions. ASCE Journal of Bridge Engineering 1996;4:127–34.
[2] Calçada R, Cunha A, Delgado R. Dynamic analysis of metallic arch railway bridge. ASCE Journal of Bridge Engineering 2002;7:214–22.
[3] Grundy P, Chitty G. Remaining life of a suite of railway bridges. IABSE Workshop: Remaining fatigue life of steel structures. Lausanne; 1990.
[4] Mang F, Bucak O. Experimental and theoretical investigations of existing railway bridges. IABSE Workshop: Remaining fatigue life of steel structures. Lausanne; 1990.
[5] Maragakis M, Douglas BM. Full-scale field failure tests of railway bridge. ASCE Journal of Bridge Engineering 2001;5:356–62.
[6] O'Connell HM, Dexter RJ. Response and analysis of steel trusses for fatigue truck loading. ASCE Journal of Bridge Engineering 2001;6: 628–38.
[7] Tobias DH, Foutch DA. Reliability-based method for fatigue evaluation of railway bridges. ASCE Journal of Bridge Engineering 1997;2:53–60.
[8] Ermopoulos J. In: Kleidarithmos, editor. Steel and composite bridges. Athens; 2000.
[9] Spyrakos CC, Kemp E, Venkatareddy R. Validated analysis of wheeling suspension bridge. ASCE Journal of Bridge Engineering 1999;4:1–7.
[10] Spyrakos CC, Kemp E, Venkatareddy R. Seismic study of an historic covered bridge. Engineering Structures 1999;21:877–82.
[11] Karydis P, Mouzakis H. In situ testing of two steel railway bridges. Earthquake Engineering Laboratory report. Athens; 1999.
[12] EBETAM SA. Chemical, metallographic, tension and fatigue tests on a steel truss railway bridge. Technical report. Volos; 2002.
[13] DIN 18800. Teil 1 ∼ 4, Stahlbauten. Berlin: Beuth Verlag GMBH, 1990.
[14] CEN European Committee for Standardization. Eurocode 3: design of steel structures—Part 1.1: General rules and rules for buildings (ENV 1993-1-1) Brussels: CEN; 1992.
[15] Spyrakos CC. Finite element modeling in engineering practice. Pittsburgh (PA): Algor Publishing Division; 1996.
[16] DS804. Vorschrift für Eisenbahnbrücken und Sonstige Ingenieurbauwerke. Deutsche Bundesbahn. 1993.
[17] Earthquake Planning and Protection Organization. Greek Aseismic Code (EAK 2000). Athens: Earthquake Planning and Protection Organization; 2000.
[18] CEN European Committee for Standardization. Eurocode 1: Actions on structures—Part 2: Traffic loads on bridges (PrEN 1991-2). Brussels: CEN; 2002.
[19] Miner MA. Cumulative damage in fatigue. ASME Journal of Applied Mechanics 1945;12(3):159–64.